Making matrices better:
Geometry and topology of polar and singular value decomposition

Dennis DeTurck, Amora Elsaify, Herman Gluck, Benjamin Grossmann
Joseph Hoisington, Anusha M. Krishnan, Jianru Zhang

Abstract

Our goal here is to see the space of matrices of a given size from a geometric and topological perspective, with emphasis on the families of various ranks and how they fit together. We pay special attention to the nearest orthogonal neighbor and nearest singular neighbor of a given matrix, both of which play central roles in matrix decompositions, and then against this visual backdrop examine the polar and singular value decompositions and some of their applications.
MSC Primary: 15-02, 15A18, 15A23, 15B10; **Secondary**: 53A07, 55-02, 57-02, 57N12, 91B24, 91G30, 92C55.

Figure 1 is the kind of picture we have in mind, in which we focus on 3×3 matrices, view them as points in Euclidean 9-space $\mathbb{R}^9$, ignore the zero matrix at the origin, and scale the rest to lie on the round 8-sphere $S^8(\sqrt{3})$ of radius $\sqrt{3}$, so as to include the orthogonal group $O(3)$.

The two components of $O(3)$ appear as real projective 3-spaces in the 8-sphere, each the core of a open neighborhood of nonsingular matrices, whose cross-sectional fibres are triangular 5-dimensional cells lying on great 5-spheres. The common boundary of these two neighborhoods is the 7-dimensional algebraic variety V^7 of singular matrices.

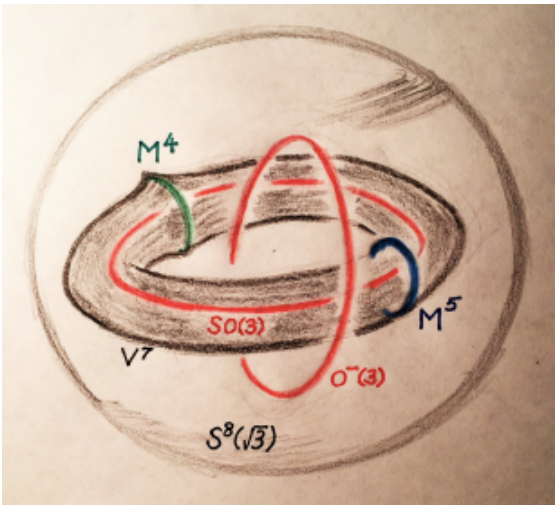

Figure 1: ***A view of 3 × 3 matrices***

This variety fails to be a submanifold precisely along the 4-manifold M^4 of matrices of rank 1. The complement $V^7 - M^4$, consisting of matrices of rank 2, is a large tubular neighborhood of a core 5-manifold M^5 consisting of the "best matrices of rank 2", namely those which are orthogonal on a 2-plane through the origin and zero on its orthogonal complement. V^7 is filled by geodesics, each an eighth of a great circle on the 8-sphere, which run between points of M^5 and M^4 with no overlap along their interiors. A circle's worth of these geodesics originate from each point of M^5, leaving it orthogonally, and a 2-torus's worth of these geodesics arrive at each point of M^4, also orthogonally.

We will confirm the above remarks, determine the topology and geometry of all these pieces, and the interesting cycles (families of matrices) which generate some of their homology, see how they all fit together to form the 8-sphere, and then in this setting visualize the polar and singular value decompositions and some of their applications.

In Figure 2, we start with a 3×3 matrix A with positive determinant on $S^8(\sqrt{3})$, and show its polar and singular value decompositions, its nearest orthogonal neighbor U, and its nearest singular neighbor B on that 8-sphere.

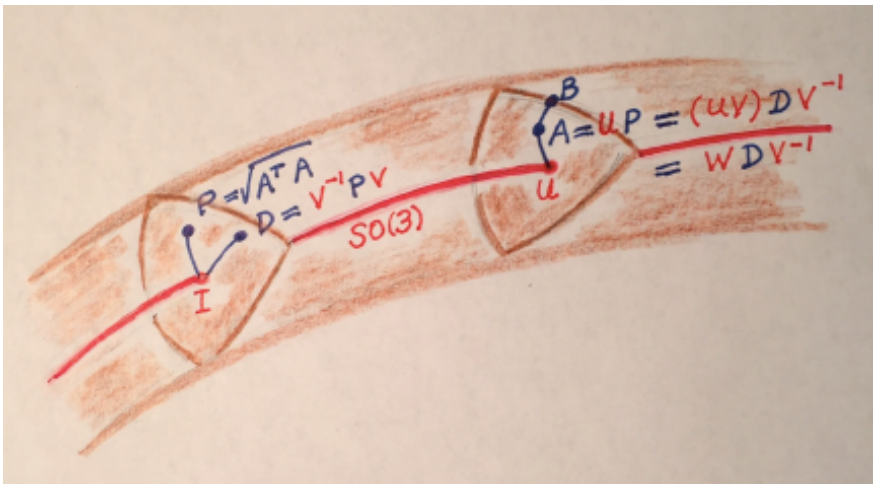

Figure 2: ***Polar and singular value decomposition of A***

Since $\det A > 0$, A lies inside the tubular neighborhood N of $SO(3)$ on the 8-sphere. The nearest orthogonal neighbor U to A is at the center of the 5-cell fibre of N containing A, while the nearest singular neighbor B to A lies on the boundary of that 5-cell.

These two nearest neighbors play a central role in the applications.

The positive definite symmetric matrix $P = \sqrt{A^T A} = U^{-1}A$ lies on the corresponding fibre of N centered at the identity I. Orthogonal diagonalization of P yields the diagonal matrix $D = V^{-1}PV$ on that same fibre, with $V \in SO(3)$.

Then we have the two matrix decompositions

$$\begin{aligned} A &= U\,P \qquad \text{(polar decomposition)} \\ &= U(VDV^{-1}) = UVDV^{-1} = WDV^{-1} \quad \text{(singular value decomposition)} \end{aligned}$$

Polar and singular value decompositions have a wealth of applications, from which we sample the following: least squares estimate of satellite attitude as well as com-

putational comparative anatomy (both instances of nearest orthogonal neighbor, and known as the ***Orthogonal Procrustes Problem***); and facial recognition via eigenfaces as well as interest rate term structures for US treasury bonds (both instances of nearest singular neighbor and known as ***Principal Component Analysis***).

To the reader.

In the first half of this paper, we focus on the geometry and topology of spaces of matrices, quickly warm up with the simple geometry of 2×2 matrices, and then concentrate entirely on the surprisingly rich and beautiful geometry of 3×3 matrices. Hoping to have set the stage well in that case, we go no further on to higher dimensions, but invite the inspired reader to do so.

In the second half of the paper, we consider matrices of arbitrary size and shape, as we focus on their singular value and polar decompositions, and applications of these, and suggest a number of references for further reading.

As usual, figures depicting higher-dimensional phenomena are at best artful lies, emphasizing some features and distorting others, and need to be viewed charitably and cooperatively by the reader.

Acknowledgments.

We are grateful to our friends Christopher Catone, Joanne Darken, Ellen Gasparovic, Chris Hays, Kostis Karatapanis, Rob Kusner and Jerry Porter for their help with this paper.

Geometry and topology of spaces of matrices

2×2 matrices

We begin with 2×2 matrices, view them as points in Euclidean 4-space $\mathbb{R}^4$, ignore the zero matrix at the origin, and scale the rest to lie on the round 3-sphere $S^3(\sqrt{2})$ of radius $\sqrt{2}$, so as to include the orthogonal group $O(2)$.

(1) First view. A simple coordinate change reveals that within this 3-sphere, the two components $SO(2)$ and $O^-(2)$ of $O(2)$ appear as linked orthogonal great circles, while the singular matrices appear as the Clifford torus halfway between these two great circles (Figure 3). The complement of this Clifford torus consists of open tubular neighborhoods N and N' of $SO(2)$ and $O^-(2)$, each an open solid torus.

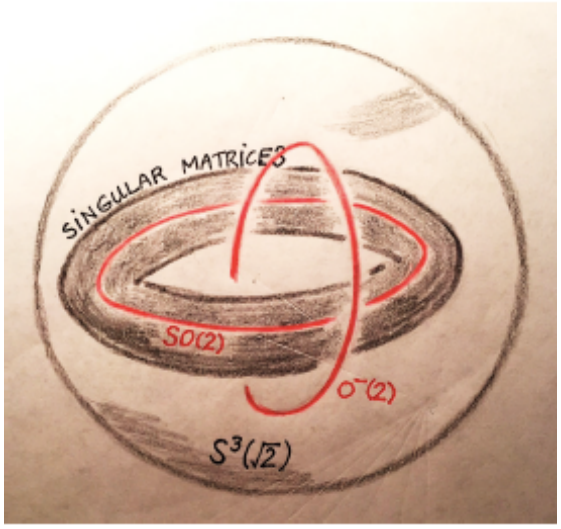

Figure 3: ***A view of 2×2 matrices***

(2) Features.

(i) On $S^3(\sqrt{2})$, the determinant function det takes its maximum value of $+1$ on $SO(2)$, its minimum value of -1 on $O^-(2)$ and its intermediate value of 0 on the Clifford torus of singular matrices.

(ii) The level sets of det on $S^3(\sqrt{2})$ are tori parallel to the Clifford torus, and the great circles $SO(2)$ and $O^-(2)$.

(iii) The orthogonal trajectories to these level sets (i.e., the gradient flow lines of det) are quarter circles which leave $SO(2)$ orthogonally and arrive at $O^-(2)$ orthogonally.

(iv) The symmetric matrices on $S^3(\sqrt{2})$ lie on a great 2-sphere with I and $-I$ as poles and with $O^-(2)$ as equator. Inside the symmetric matrices, the diagonal matrices appear as a great circle through these poles, passing alternately through the tubular neighborhoods N and N' of $SO(2)$ and $O^-(2)$, and crossing the Clifford torus four times.

(v) On the great 2-sphere of symmetric matrices, the round disk of angular radius $\pi/4$ centered at I is one of the cross-sectional fibres of the tubular neighborhood N of $SO(2)$. It meets $SO(2)$ orthogonally at its center, and meets the Clifford torus orthogonally along its boundary, thanks to (i), (ii) and (iii) above.

(vi) The tangent space to $S^3(\sqrt{2})$ at the identity matrix I decomposes orthogonally into the one-dimensional space of skew-symmetric matrices (tangent to $SO(2)$), and the two-dimensional space of traceless symmetric matrices, tangent to the great 2-sphere of symmetric matrices. Within the traceless symmetric matrices is the one-dimensional space of traceless diagonal matrices, tangent to the great circle of diagonal matrices.

(vii) Left or right multiplication by elements of $SO(2)$ are isometries of $S^3(\sqrt{2})$ which take this cross-sectional fibre of N at I to the corresponding cross-sectional fibres of N at the other points along $SO(2)$. Left or right multiplication by elements of $O^-(2)$ take this fibration of N to the corresponding fibration of N'.

(3) Nearest orthogonal neighbor. Start with a nonsingular 2×2 matrix A on $S^3(\sqrt{2})$ and suppose, to be specific, that A lies in the open tubular neighborhood N of $SO(2)$. ***We claim that the nearest orthogonal neighbor to A on that 3-sphere is the center of the cross-sectional fibre of N on which it lies.***

To see this, note that a geodesic (great circle arc) from A to its nearest neighbor U on $SO(2)$ must meet $SO(2)$ orthogonally at U, and therefore must lie in the cross-sectional fibre of N through U. It follows that A also lies in that fibre, whose center is at U, confirming the above claim.

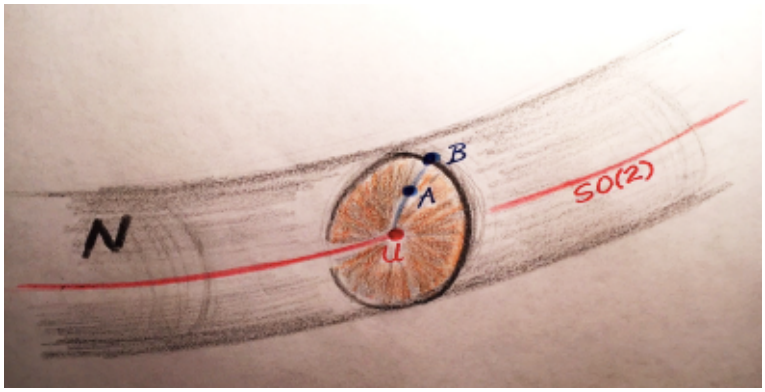

Figure 4: ***Nearest orthogonal and nearest singular neighbors to a matrix A***

(4) Nearest singular neighbor. Start with a nonsingular 2×2 matrix A on $S^3(\sqrt{2})$. ***We claim that the nearest singular neighbor to A on that 3-sphere is on the boundary of the cross-sectional disk on which it lies, at the end of the ray from its center through A.***

To see this, recall from (1) that the level surfaces of det on $S^3(\sqrt{2})$ are tori parallel to the Clifford torus, and that their orthogonal trajectories are the quarter circles

which leave $SO(2)$ orthogonally and arrive at $O^-(2)$ orthogonally. It follows that the geodesics orthogonal to the Clifford torus lie in the cross-sectional disk fibres of the tubular neighborhoods N and N' of $SO(2)$ and $O^-(2)$.

Now a geodesic (great circle arc) from A to its nearest singular neighbor B on the Clifford torus must meet that torus orthogonally at B, and hence must lie in one of these cross-sectional disk fibres (Figure 4). If A is not orthogonal, then B lies at the end of the unique ray from the center of this fibre through A, and hence is uniquely determined by A. If A is orthogonal, then B can lie at the end of any of the rays from the center A of this fibre, and so every point on the circular boundary of this fibre is a closest singular neighbor to A on $S^3(\sqrt{2})$.

(5) Gram-Schmidt. Having just looked at the geometrically natural map which takes a nonsingular 2×2 matrix to its nearest neighbor on the orthogonal group $O(2)$, it is irresistable to compare this with the Gram-Schmidt orthonormalization procedure. This procedure depends on a choice of basis for $\mathbb{R}^2$, hence is not "geometrically natural", that is to say, not $O(2) \times O(2)$ equivariant.

We see this geometric defect in Figure 5, where we restrict the Gram-Schmidt procedure GS to $S^3(\sqrt{2})$, and display the inverse image $GS^{-1}(I)$ of the identity I on that 3-sphere.

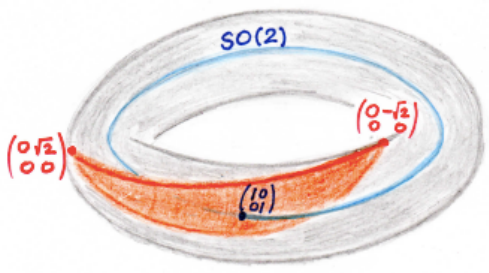

Figure 5: ***$GS^{-1}(I)$ is an open 2-cell in $S^3(\sqrt{2})$ with boundary on the Clifford torus***

The inverse images of the other points on $SO(2)$ are rotated versions of $GS^{-1}(I)$. It is visually evident that this picture, and hence the Gram-Schmidt procedure itself, is not equivariant with respect to the action of $SO(2)$ via conjugation, which fixes $SO(2)$ pointwise, but rotates $O^-(2)$ within itself.

3×3 matrices

We turn now to 3×3 matrices, view them as points in Euclidean 9-space $\mathbb{R}^9$, once again ignore the zero matrix at the origin, and scale the rest to lie on the round 8-sphere $S^8(\sqrt{3})$ of radius $\sqrt{3}$, so as to include the orthogonal group $O(3)$.

(1) First view. The two components $SO(3)$ and $O^-(3)$ of $O(3)$ appear as real projective 3-spaces on $S^8(\sqrt{3})$, while the singular matrices (ranks 1 and 2) on this 8-sphere appear as a 7-dimensional algebraic variety V^7 separating them.

Contrary to appearances in Figure 6, the two components of $O(3)$ are too low-dimensional to be linked in the 8-sphere. The subspaces V^7, M^4 and M^5 in the figure were defined in the introduction, and will be examined in detail as we proceed.

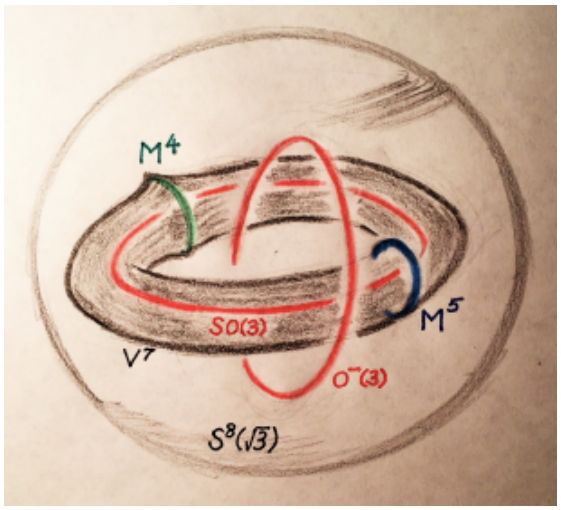

Figure 6: ***A view of 3 × 3 matrices***

(2) The tangent space to $S^8(\sqrt{3})$ at the identity matrix decomposes orthogonally into the three-dimensional space of skew-symmetric matrices (tangent to $SO(3)$), and the five-dimensional space of traceless symmetric matrices, tangent to the great 5-sphere of symmetric matrices. Within the traceless symmetric matrices is the two-dimensional space of traceless diagonal matrices, tangent to the great 2-sphere of diagonal matrices in $S^8(\sqrt{3})$.

(3) A 2-sphere's worth of diagonal 3×3 matrices. The great 2-sphere of diagonal 3×3 matrices on $S^8(\sqrt{3})$ will play a key role in our understanding of the geometry of 3×3 matrices as a whole.

In Figure 7, the diagonal matrix $\mathrm{diag}(x, y, z)$ is located at the point (x, y, z), and indicated "distances" are really angular separations.

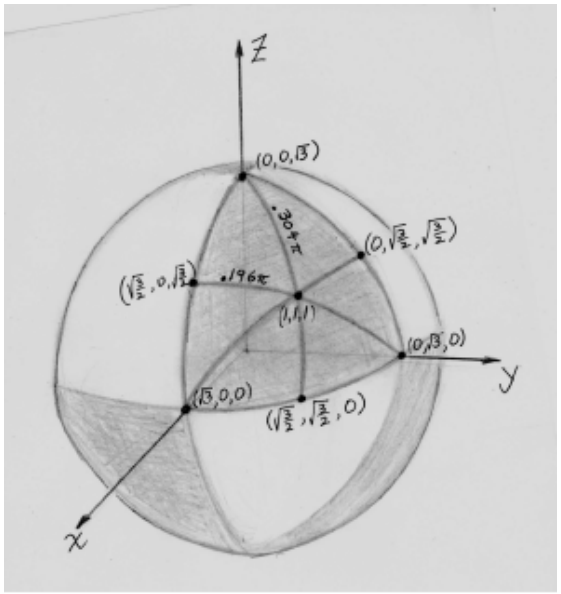

Figure 7: ***Diagonal matrices in $S^8(\sqrt{3})$***

This 2-sphere is divided into eight spherical triangles, with the shaded ones centered at the points $(1, 1, 1)$, $(-1, -1, 1)$, $(1, -1, -1)$ and $(-1, 1, -1)$ of $SO(3)$, and the unshaded ones centered at points of $O^-(3)$.

The interiors of the shaded triangles will lie in the open tubular neighborhood (yet to be defined) of $SO(3)$ on $S^8(\sqrt{3})$, the interiors of the unshaded triangles will lie in the open tubular neighborhood of $O^-(3)$, while the shared boundaries lie on the variety V^7 of singular matrices, with the vertices of rank 1, the open edges of rank 2, and the centers of the edges "best of rank 2".

(4) Symmetries. We have $O(3) \times O(3)$ acting as a group of isometries of our space $\mathbb{R}^9$ of all 3×3 matrices, and hence of the normalized ones on $S^8(\sqrt{3})$, via the map

$$(U, V) * A = UAV^{-1}.$$

This action is a rigid motion of the 8-sphere which takes the union of the two $\mathbb{R}P^3$s representing $O(3)$ to themselves (possibly interchanging them), and takes the variety V^7 of singular matrices separating them to itself.

"Natural geometric constructions" for 3×3 matrices are those which are equivariant with respect to this action of $O(3) \times O(3)$.

(5) Tubular neighborhoods of $SO(3)$ and $O^-(3)$ in $S^8(\sqrt{3})$. We expect, by analogy with 2×2 matrices, that the complement in $S^8(\sqrt{3})$ of the variety V^7 of singular matrices consists of open tubular neighborhoods of the two components $SO(3)$ and $O^-(3)$ of the orthogonal group, with fibres which lie on the great 5-spheres which meet these cores orthogonally.

At the same time, our picture of the great 2-sphere's worth of diagonal 3×3 matrices alerts us that we cannot expect the fibres of these neighborhoods to be round 5-cells; instead they must somehow take on the triangular shapes seen in Figure 7.

Indeed, look at that figure and focus on the open shaded spherical triangle D^2 centered at the identity and lying in the first octant. Let $SO(3)$ act on this triangle by conjugation,

$$A \to U * A = UAU^{-1},$$

and the image will be a corresponding open triangular shaped region D^5 centered at the identity on the great 5-sphere of symmetric matrices, and consisting of the positive definite ones. Going from D^2 to D^5 is like fluffing up a pillow.

This open 5-cell D^5 is the fibre centered at the identity of the tubular neighborhood N of $SO(3)$, and the remaining fibres can be obtained by left (say) translation of D^5 by the elements of $SO(3)$.

Why are these fibres disjoint? That is, why will two left translates of D^5 along $SO(3)$ be disjoint?

We can see from Figure 7 that it is going to be a close call, since the ***closures*** of the spherical triangles centered at $(1, 1, 1)$ and at $(1, -1, -1)$ meet at the point $(\sqrt{3}, 0, 0)$, even though their interiors are disjoint.

Consider a closed geodesic on $SO(3)$, such as the set of transformations

$$A_t = \begin{bmatrix} \cos t & -\sin t & 0 \\ \sin t & \cos t & 0 \\ 0 & 0 & 1 \end{bmatrix} \qquad 0 \le t \le 2\pi.$$

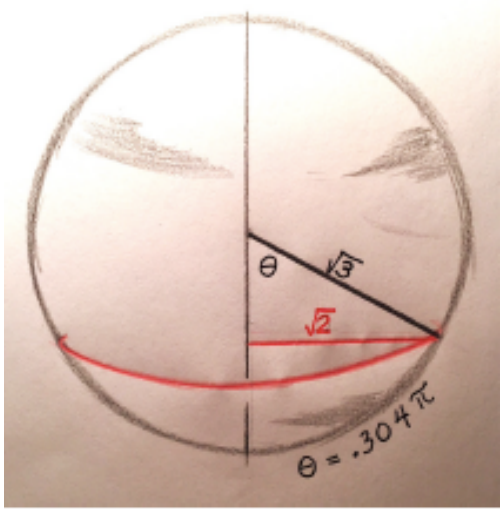

Figure 8: ***A closed geodesic on SO(3) appears as a small circle on $S^8(\sqrt{3})$***

Figure 8 is a picture of that closed geodesic, appearing as a small circle of radius $\sqrt{2}$ on $S^8(\sqrt{3})$.

In this picture, two great circles which meet the small circle orthogonally will come together at the south pole, after traveling an angular distance $0.304\,\pi$, but not before.

Since any two points U and V of $SO(3)$ lie together on a common closed geodesic (which is a small circle of radius $\sqrt{2}$ on an 8-sphere of radius $\sqrt{3}$), and since the maximum angular separation between the center of the 5-disk D^5 and its boundary is $0.304\,\pi$, it follows that the ***open*** 5-disks UD^5 and VD^5 must be disjoint.

In this way, we see that the union of the disjoint open 5-disks UD^5, as U ranges over $SO(3)$, forms an open tubular neighborhood N of $SO(3)$ in $S^8(\sqrt{3})$. This tubular neighborhood is topologically trivial under the map

$$SO(3) \times D^5 \to N \quad \text{via} \quad (U, P) \to UP.$$

In similar fashion, we get an open tubular neighborhood N' of $O^-(3)$, likewise topologically trivial. The common boundary of these two tubular neighborhoods is the variety V^7 of singular matrices on $S^8(\sqrt{3})$.

(6) The determinant function on $S^8(\sqrt{3})$. The determinant function det on $S^8(\sqrt{3})$ takes its maximum value of $+1$ on $SO(3)$, its minimum value of -1 on $O^-(3)$, and its intermediate value of 0 on V^7.

Unlike the situation for 2×2 matrices, the orthogonal trajectories of the level sets of det are not geodesics, since the 5-cell fibres of the tubular neighborhoods N and N' of $SO(3)$ and $O^-(3)$ are not round. In Figure 9, we see the level curves of det on the great 2-sphere of diagonal matrices.

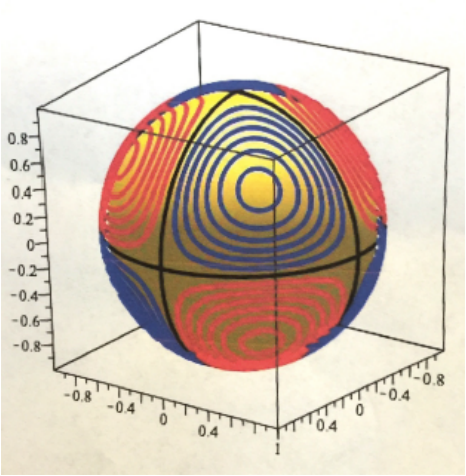

Figure 9: ***Level curves of* det *on the* 2*-sphere of diagonal matrices***

(7) The 7-dimensional variety V^7 of singular matrices on $S^8(\sqrt{3})$. The singular 3×3 matrices A on $S^8(\sqrt{3})$ fill out a 7-dimensional algebraic variety V^7 defined by the equations $\|A\|^2 = 3 \quad \text{and} \quad \det A = 0$. Nothing in our warmup with 2×2 matrices prepares us for the incredible richness in the geometry and topology of this variety, which is sketched in Figure 10.

At the lower left is the 4-manifold M^4 of matrices of rank 1, along which V^7 fails to be a manifold, and at the upper right is the 5-manifold M^5 of best matrices of rank 2 .

The little torus linking M^4 signals (in advance of proof) that a torus's worth of geodesics on V^7 shoot out orthogonally from each of its points, while the little circle linking M^5 signals that a circle's worth of geodesics on V^7 shoot out orthogonally from each of its points.

These are the same geodesics, each an eighth of a great circle, and they fill V^7 with no overlap along their interiors.

(8) What portion of V^7 is a manifold? Identifying the set of all 3×3 matrices with Euclidean space $\mathbb{R}^9$, we consider the determinant function $\det\colon \mathbb{R}^9 \to \mathbb{R}$.

Let $A = (a_{rs})$ be a given 3×3 matrix. Then one easily computes the gradient of the determinant function to be

$$(\nabla \det)_A = \sum_{r,s} A_{rs} \frac{\partial}{\partial a_{rs}},$$

where A_{rs} is the cofactor of a_{rs} in A.

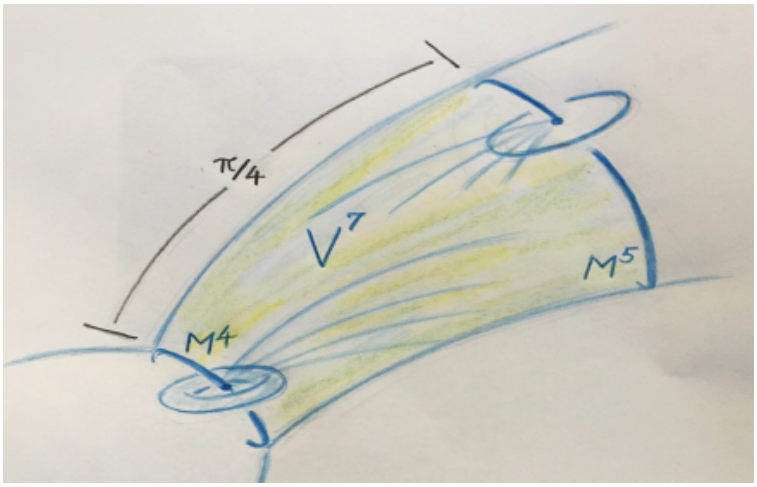

Figure 10: ***The variety V^7 of singular 3×3 matrices***

Thus $(\nabla \det)_A$ vanishes if and only if all the 2×2 cofactors of A vanish, which happens only when A has rank ≤ 1.

The subvariety V^7 of $S^8(\sqrt{3})$ consisting of the singular matrices is the zero set of the determinant function $\det\colon S^8(\sqrt{3}) \to \mathbb{R}$.

If A is a matrix of rank 2 on V^7 then $\det A = 0$ and the gradient vector $(\nabla \det)_A$ is nonzero there, when det is considered as a function from $\mathbb{R}^9 \to \mathbb{R}$. Since $\det(tA) = 0$ for all real numbers t, the vector $(\nabla \det)_A$ must be orthogonal to the ray through A, and hence tangent to $S^8(\sqrt{3})$. Therefore $(\nabla \det)_A$ is also nonzero when det is considered as a function from $S^8(\sqrt{3}) \to \mathbb{R}$. It follows that V^7 is a submanifold of $S^8(\sqrt{3})$ at all its points A of rank 2.

But V^7 fails to be a manifold at all its points of rank 1, that is, along the subset M^4, as we will confirm shortly.

(9) The 5-cell fibres of N and N' meet V^7 orthogonally along their boundaries. This was noted earlier for 2×2 matrices on $S^3(\sqrt{2})$.

Lemma 1. ***On $S^8(\sqrt{3})$, the gradient vector field of the determinant function, when evaluated at a diagonal matrix, is tangent to the great 2-sphere of diagonal matrices.***

Proof. Looking once again at the gradient of the determinant function,

$$(\nabla \det)_A = \sum_{r,s} A_{rs} \frac{\partial}{\partial a_{rs}},$$

where A_{rs} is the cofactor of a_{rs} in A, we see that if A is a diagonal matrix, then $(\nabla \det)_A$ is tangent to the space of diagonal matrices because each off-diagonal cofactor is zero, and if A lies on $S^8(\sqrt{3})$, then the projection of $(\nabla \det)_A$ to $S^8(\sqrt{3})$ is still tangent to the space of diagonal matrices there.

Lemma 2. ***More generally, this gradient field is tangent to the* 5*-dimensional cross-sectional cells of the tubular neighborhoods* N *and* N' *of* $SO(3)$ *and* $O^-(3)$*.***

Proof. If D^2 is the 2-dimensional cell of diagonal matrices in the tubular neighborhood N of $SO(3)$ on $S^8(\sqrt{3})$, then its isometric images UD^2U^{-1}, as U ranges over $SO(3)$, fill out the cross-sectional 5-cell D^5 of N at the identity I. Since the determinant function is invariant under this conjugation, its gradient is equivariant, and so must be tangent to this D^5 at each of its points. Then, using left translation by elements of $SO(3)$, we see that the gradient field is tangent to ***all*** the cross-sectional 5-cells of N ... and likewise for N'.

Proposition 3. ***The cross-sectional* 5*-cell fibres of the tubular neighborhoods* N *and* N' *of* $SO(3)$ *and* $O^-(3)$ *on* $S^8(\sqrt{3})$ *meet the variety* V^7 *of singular matrices orthogonally at their boundaries.***

Proof. The gradient vector field of the determinant function on $S^8(\sqrt{3})$ is orthogonal to the level surface V^7 of this function, and at the same time it is tangent to the cross-sectional 5-cell fibres of N and N'. So it follows that these 5-cell fibres meet V^7 orthogonally at their boundaries.

(10) The submanifold M^4 of matrices of rank 1. First we identify M^4 as a manifold. Define $S^2 \otimes S^2$ to be the quotient of $S^2 \times S^2$ by the equivalence relation $(x, y) \sim (-x, -y)$, a space which is (coincidentally) also homeomorphic to the Grassmann manifold of unoriented 2-planes through the origin in real 4-space. It is straightforward to confirm that M^4 is homeomorphic to $S^2 \otimes S^2$.

Define a map $f\colon S^2 \times S^2 \to M^4$ by sending the pair of points $\mathbf{x} = (x_1, x_2, x_3)$ and $\mathbf{y} = (y_1, y_2, y_3)$ on $S^2 \times S^2$ to the 3×3 matrix $(x_r y_s)$, scaled up to lie on $S^8(\sqrt{3})$. Then check that this map is onto, and that the only duplication is that $(\mathbf{x}, \mathbf{y})$ and $(-\mathbf{x}, -\mathbf{y})$ go to the same matrix.

Remarks. (1) M^4 is an ***orientable*** manifold because the involution $(\mathbf{x}, \mathbf{y}) \to (-\mathbf{x}, -\mathbf{y})$ of $S^2 \times S^2$ is orientation-preserving.

(2) M^4 is a single orbit of the $O(3) \times O(3)$ action.

(3) The integer homology groups of M^4 are

$$H_0(M^4) = \mathbb{Z}, \quad H_1(M^4) = \mathbb{Z}_2, \quad H_2(M^4) = \mathbb{Z}_2, \quad H_3(M^4) = 0 \quad \text{and} \quad H_4(M^4) = \mathbb{Z},$$

an exercise in using Euler characteristic and Poincaré duality (Hatcher [2002]). Thus M^4 has the same ***rational*** homology as the 4-sphere S^4.

(11) Tangent and normal vectors to M^4. At the point $P = \mathrm{diag}(\sqrt{3}, 0, 0)$, the tangent and normal spaces to M^4 within $S^8(\sqrt{3})$ are

$$T_P M^4 = \left\{ \begin{bmatrix} 0 & a & b \\ c & 0 & 0 \\ d & 0 & 0 \end{bmatrix} \; a, b, c, d \in \mathbb{R} \right\} \quad \text{and} \quad (T_P M^4)^\perp = \left\{ \begin{bmatrix} 0 & 0 & 0 \\ 0 & a & b \\ 0 & c & d \end{bmatrix} \; a, b, c, d \in \mathbb{R} \right\}$$

We leave this to the interested reader to confirm.

(12) The singularity of V^7 along M^4. Let $A = \begin{bmatrix} a & b \\ c & d \end{bmatrix}$ be a 2×2 matrix with $a^2 + b^2 + c^2 + d^2 = 1$. Then a geodesic (i.e., great circle) $\gamma(t)$ on $S^8(1)$ which runs through the rank 1 matrix $P = \mathrm{diag}(1, 0, 0)$ at time $t = 0$, and is orthogonal there to M^4 has the form

$$\gamma(t) = \begin{bmatrix} \cos t & 0 & 0 \\ 0 & a \sin t & b \sin t \\ 0 & c \sin t & d \sin t \end{bmatrix}, \quad \text{with} \quad \gamma'(0) = \begin{bmatrix} 0 & 0 & 0 \\ 0 & a & b \\ 0 & c & d \end{bmatrix}.$$

If the 2×2 matrix A above has rank 2, then $\gamma(t)$ immediately has rank 3 for small $t > 0$. But if A has rank 1, then $\gamma(t)$ has only rank 2 for small $t > 0$.

We know from our study of 2×2 matrices that those of rank 1 form a cone (punctured at the origin) over the Clifford torus in $S^3(1)$. Thus the tubular neighborhood of M^4 in V^7 is a bundle over M^4 whose normal fibre is a cone over the Clifford torus. We indicate this pictorially in Figure 11.

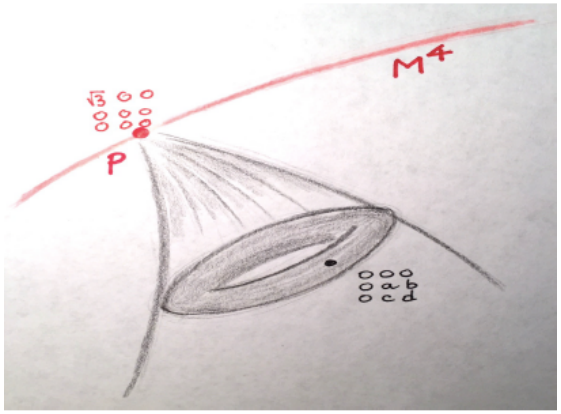

Figure 11: ***The normal cone to M^4 in V^7 at the point P is a cone over a Clifford torus $a^2 + b^2 + c^2 + d^2 = 1$ and $ad - bc = 0$***

One can use the information above to show that

(1) $V^7 - M^5$ is a "tubular" neighborhood of M^4, whose cross-sections are great circle cones of angular radius $\pi/4$ over Clifford tori on great 3-spheres which meet M^4 orthogonally.

(2) The 2-torus's worth of geodesic rays shooting out from each point of M^4 in V^7 terminate along a full 2-torus's worth of points in M^5.

(13) The submanifold M^5 = {Best of rank 2}. Recall that the "best" 3×3 matrices of rank 2 are those which are orthogonal on a 2-plane through the origin, and zero on its orthogonal complement.

An example of such a matrix is $P = \mathrm{diag}(1,1,0) = \begin{bmatrix} 1 & 0 & 0 \\ 0 & 1 & 0 \\ 0 & 0 & 0 \end{bmatrix}$, representing orthogonal projection of xyz-space to the xy-plane.

We let M^5 denote the set of best 3×3 matrices of rank 2, scaled up to lie on $S^8(\sqrt{3})$. This set is a single orbit of the $SO(3) \times SO(3)$ action on $\mathbb{R}^9$.

Claim: *M^5 is homeomorphic to $\mathbb{R}P^2 \times \mathbb{R}P^3$.*

Proof. Let T be one of these best 3×3 matrices of rank 2 . Then the kernel of T is some unoriented line through the origin in $\mathbb{R}^3$, hence an element of $\mathbb{R}P^2$.

An orthogonal transformation of $(\ker T)^\perp$ to a 2-plane through the origin in $\mathbb{R}^3$ can be uniquely extended to an orientation-preserving orthogonal transformation A_T of $\mathbb{R}^3$ to itself, hence an element of $SO(3)$.

Then the correspondence $T \to (\ker T\,,\, A_T)$ gives the homeomorphism of M^5 with $\mathbb{R}P^2 \times SO(3)$, equivalently, with $\mathbb{R}P^2 \times \mathbb{R}P^3$.

Remark. M^5 is non-orientable, and its integer homology groups are

$$H_0(M^5) = \mathbb{Z}, \quad H_1(M^5) = \mathbb{Z}_2 + \mathbb{Z}_2, \quad H_2(M^5) = \mathbb{Z}_2, \quad H_3(M^5) = \mathbb{Z} + \mathbb{Z}_2,$$
$$H_4(M^5) = \mathbb{Z}_2, \quad H_5(M^5) = 0,$$

an exercise in using the Künneth formula (Hatcher [2002]) for the homology of a product.

(14) Tangent and normal vectors to M^5. At the point $P = \mathrm{diag}\left(\sqrt{\tfrac{3}{2}}\,,\, \sqrt{\tfrac{3}{2}}\,,\, 0\right)$, the tangent and normal spaces to M^5 within V^7 are

$$T_P M^5 = \left\{ \begin{bmatrix} 0 & -a & b \\ a & 0 & c \\ d & e & 0 \end{bmatrix} \;\; a,b,c,d,e \in \mathbb{R} \right\} \quad \text{and} \quad (T_P M^5)^\perp = \left\{ \begin{bmatrix} a & b & 0 \\ b & -a & 0 \\ 0 & 0 & 0 \end{bmatrix} \;\; a,b \in \mathbb{R} \right\}$$

and $(T_P V^7)^\perp \subset T_P S^8(\sqrt{3})$ is spanned by $\mathrm{diag}(0,0,1)$, as the reader can confirm.

(15) The tubular neighborhood of M^5 inside V^7 .

Claim: *$V^7 - M^4$ is a tubular neighborhood of M^5, whose cross sections are round cells of angular radius $\pi/4$ on great 2-spheres which meet M^5 orthogonally.*

Proof. We start on M^5 at the scaled point $P = \mathrm{diag}(1,1,0) = \begin{bmatrix} 1 & 0 & 0 \\ 0 & 1 & 0 \\ 0 & 0 & 0 \end{bmatrix}$, which represents orthogonal projection of xyz-space to the xy-plane. Then we consider the tangent vectors

$$T_1 = \begin{bmatrix} 0 & 1 & 0 \\ 1 & 0 & 0 \\ 0 & 0 & 0 \end{bmatrix} \quad \text{and} \quad T_2 = \begin{bmatrix} 1 & 0 & 0 \\ 0 & -1 & 0 \\ 0 & 0 & 0 \end{bmatrix}$$

which are an orthogonal basis for $(T_P M^5)^\perp \subset T_P V^7$.

If we exponentiate the vector in $(T_P M^5)^\perp$ given by $aT_1 + bT_2$, with $a^2 + b^2 = 1$, from the point P, we get

$$P(t) = (\cos t)P + (\sin t)(aT_1 + bT_2) = \begin{bmatrix} \cos t + b\sin t & a\sin t & 0 \\ a\sin t & \cos t - b\sin t & 0 \\ 0 & 0 & 0 \end{bmatrix}$$

which has rank 2 for $0 \le t < \pi/4$. All these matrices have the same kernel and same image as P . But $P(\pi/4) = \dfrac{1}{\sqrt{2}} \begin{bmatrix} 1+b & a & 0 \\ a & 1-b & 0 \\ 0 & 0 & 0 \end{bmatrix}$, which only has rank 1, and therefore lies on M^4.

The set of points $\{P(t) : 0 \le t \le \pi/4\}$ is one-eighth of a great circle on $S^8(\sqrt{3})$, beginning at the point $P = P(0)$ on M^5 and ending at the point $P(\pi/4)$ on M^4. Let's call this set a ***ray***.

We see from the entries in the above matrix that the circle's worth of rays shooting out from the point P orthogonal to M^5 in V^7 terminate along a full circle's worth of points on M^4. We can think of this as an "absence of focusing".

Since M^5 is a single orbit of the $SO(3) \times SO(3)$ action on $\mathbb{R}^9$, the above situation at the point P on M^5 is replicated at every point of M^5, confirming the claim made above.

(16) The wedge norm on V^7. Recall that for 2×2 matrices viewed as points in $\mathbb{R}^4$ and then restricted to $S^3(\sqrt{2})$, the determinant function varies between a maximum

of 1 on $SO(2)$ and a minimum of -1 on $O^-(2)$, with the middle value zero assumed on the Clifford torus of singular matrices. The level sets of this for values strictly between -1 and 1 are tori parallel to the Clifford torus, and are principal orbits of the $SO(2) \times SO(2)$ action. Their orthogonal trajectories are the geodesic arcs leaving $SO(2)$ orthogonally and arriving at $O^-(2)$ orthogonally a quarter of a great circle later.

We seek a corresponding function on the variety V^7 of singular matrices on $S^8(\sqrt{3})$, whose level sets fill the space between M^4 and M^5, and to this end, turn to the wedge norm $\|A \wedge A\|$, defined as follows.

If $A\colon V \to W$ is a linear map between the real vector spaces V and W, then the induced linear map $A \wedge A\colon \wedge^2 V \to \wedge^2 W$ between spaces of 2-vectors is defined by

$$(A \wedge A)(\mathbf{v}_1 \wedge \mathbf{v}_2) = A(\mathbf{v}_1) \wedge A(\mathbf{v}_2),$$

with extension by linearity. If $V = W = \mathbb{R}^2$, then the space $\wedge^2\mathbb{R}^2$ is one-dimensional, and $A \wedge A$ is simply multiplication by $\det A$, while if $V = W = \mathbb{R}^3$, then the space $\wedge^2\mathbb{R}^3$ is three-dimensional, and $A \wedge A$ coincides with the matrix of cofactors of A.

The wedge norm is defined by $\|A \wedge A\|^2 = \sum_{i,j}(A \wedge A)_{ij}^2$, and is easily seen to be $SO(3) \times SO(3)$-invariant, and thus constant along the orbits of this action. It has the following properties:

(1) On V^7 the wedge norm takes its maximum value of $3/2$ on M^5 and its minimum value of 0 on M^4.

(2) The level sets between these two extreme values are 6-dimensional submanifolds which are principal orbits of the $SO(3) \times SO(3)$ action.

(3) The orthogonal trajectories of these level sets are geodesic arcs, each an eighth of a great circle, meeting both M^4 and M^5 orthogonally.

(17) Concrete generators for the 4-dimensional homology of V^7. If we remove both components of the orthogonal group $O(3)$ from the 8-sphere $S^8(\sqrt{3})$, then what is left over deformation retracts to the variety V^7, since each cross-sectional 5-cell D^5 in the tubular neighborhoods of these two components has now had its center removed, and so can deformation retract to its boundary along great circle arcs.

Therefore V^7 has the same integer homology as $S^8(\sqrt{3}) - O(3)$, which can be computed by Alexander duality (Hatcher [2002]), and we learn that

$$H_0(V^7) = \mathbb{Z}, \quad H_4(V^7) = \mathbb{Z} + \mathbb{Z}, \quad H_5(V^7) = \mathbb{Z}_2 + \mathbb{Z}_2, \quad H_7(V^7) = \mathbb{Z},$$

while the remaining homology groups are zero. The variety V^7 is orientable because it divides $S^8(\sqrt{3})$ into two components, but its homology is excused from satisfying Poincaré duality because it is not a manifold.

We seek concrete cycles generating $H_4(V^7)$.

Pick a point on each component of $O(3)$, for example, the identity I on $SO(3)$, and $-I$ on $O^-(3)$. Then go out a short distance in the cross-sectional 5-cells of the two tubular neighborhoods, and we will have a pair of 4-spheres, each linking the corresponding component of $O(3)$, and therefore generating $H_4(S^8(\sqrt{3}) - O(3))$. Pushing these 4-spheres outwards to V^7 along the great circle rays of these two 5-cells provides the desired generators for $H_4(V^7)$.

How are these generators positioned on V^7?

The key to the answer can be found in the diagonal 3×3 matrices. In Figure 12, consider the spherical triangle centered at $(1, 1, 1)$. We noted earlier that the three vertices of this triangle lie in M^4, and the centers of its three edges in M^5. The six half-edges are geodesics, each an eighth of a great circle.

Conjugating by $SO(3)$ promotes this triangle to the cross-sectional 5-cell centered at the identity in the tubular neighborhood of $SO(3)$, and promotes the decomposition of the boundary of the triangle to a decomposition of the boundary $+S^4$ of this 5-cell.

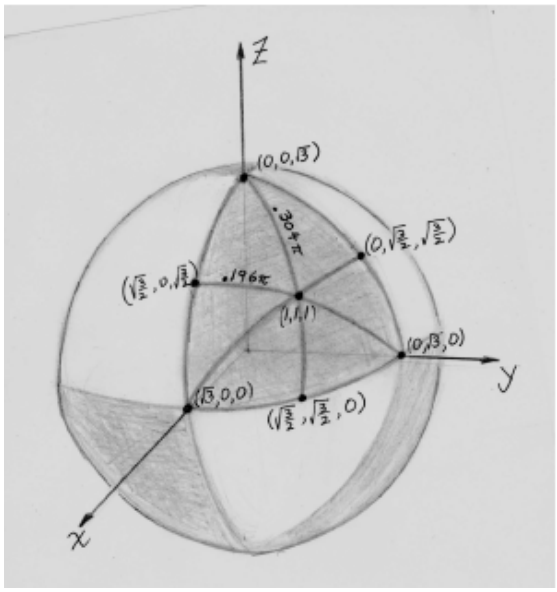

Figure 12: ***Diagonal matrices in $S^8(\sqrt{3})$***

This is enough to reveal the positions of our two generators of $H_4(V^7)$. We show this in Figure 13, where

(1) The lower 4-sphere $+S^4$ links $SO(3)$ in $S^8(\sqrt{3})$, and is the set of symmetric positive semi-definite matrices there which are not positive definite.

(2) The upper 4-sphere $-S^4$ links $O^-(3)$, and is the set of symmetric negative semi-definite matrices on $S^8(\sqrt{3})$ which are not negative definite.

(3) Each of these 4-spheres has an $\mathbb{R}P^2$ end in M^4 and another $\mathbb{R}P^2$ end in M^5, and is smooth, except at the end in M^4.

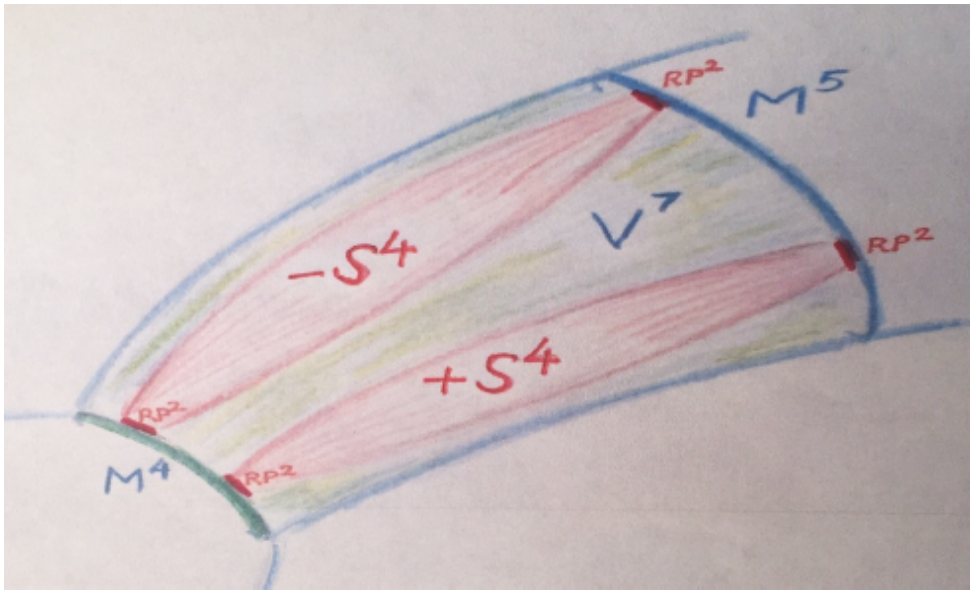

Figure 13: ***Generators of $H_4(V^7)$ are 4-spheres with $\mathbb{R}P^2$ ends in M^4 and M^5***

(4) The $SO(3)$ action by conjugation on each 4-sphere is the same as that on the unit 4-sphere in the space of traceless, symmetric 3×3 matrices described by Blaine Lawson [1980] . The principal orbits are all copies of the group S^3 of unit quaternions, modulo its subgroup $\{\pm 1, \pm i, \pm j, \pm k\}$, the singular orbits are the $\mathbb{R}P^2$ ends, and the orthogonal trajectories are geodesic arcs, each an eighth of a great circle.

(18) Nearest orthogonal neighbor. Start with a nonsingular 3×3 matrix A on $S^8(\sqrt{3})$ and suppose, to be specific, that A lies in the open tubular neighborhood N of $SO(3)$.

We claim that the nearest orthogonal neighbor to A on that 8-sphere is the center of the cross-sectional fibre of N on which it lies.

To see this, note that a geodesic (great circle arc) from A to its nearest neighbor U on $SO(3)$ must meet $SO(3)$ orthogonally at U, and therefore must lie in the cross-sectional fibre of N through U. It follows that A also lies in that fibre, whose center is at U, confirming the above claim.

(19) Nearest singular neighbor. Start with a nonsingular 3×3 matrix A on $S^8(\sqrt{3})$, say with $\det A > 0$.

We claim that the nearest singular neighbor to A on that 8-sphere lies on the boundary of the cross-sectional 5-cell of the tubular neighborhood N of $SO(3)$ which contains A.

Lemma. ***Let A be a nonsingular 3×3 matrix on $S^8(\sqrt{3})$, and let B be the closest singular matrix to A on this 8-sphere. Then B has rank 2.***

Proof. Suppose B has rank 1, and therefore lies in M^4. Since $SO(3) \times SO(3)$ acts transitively on M^4, we can choose orthogonal matrices U and V so that $UBV^{-1} = \mathrm{diag}(\sqrt{3}, 0, 0)$, and this will then be the closest singular matrix to the nonsingular matrix UAV^{-1}. So we can assume that $B = \mathrm{diag}(\sqrt{3}, 0, 0)$ already.

Since A is nonsingular, it must have at least one nonzero entry a_{ij} for some $i > 1$ and $j > 1$. Now let T be the matrix with all zeros except in the ijth spot, with $t_{ij} = \mathrm{sgn}(a_{ij})\sqrt{3}$. Then T also lies on $S^8(\sqrt{3})$ and is orthogonal to B.

Hence the matrices $B(t) = \cos t\, B + \sin t\, T$ lie on $S^8(\sqrt{3})$ as well, and

$$\langle A, B(t)\rangle = \cos t\, \langle A, B\rangle + \sin t\, \langle A, T\rangle.$$

The derivative of this inner product with respect to t at $t = 0$ is

$$\langle A, T\rangle = |a_{ij}|\sqrt{3} > 0.$$

Therefore, for small values of t, $B(t)$ is a matrix of rank 2 on $S^8(\sqrt{3})$ that is closer to A than B was. This contradicts the assumption that B was closest to A, and proves the lemma.

Remarks. (1) For visual evidence in support of this lemma, look at the front shaded spherical triangle on the great 2-sphere of diagonal 3×3 matrices in Figure 12, and note that if A is an interior point of this triangle, then the closest boundary point B cannot be one of the vertices.

(2) More generally, let A be an $n \times n$ matrix of rank $> r$ on S^{n^2-1}. Then the matrix B on S^{n^2-1} of rank $\leq r$ that is closest to A actually has rank r.

Now given the nonsingular matrix A on $S^8(\sqrt{3})$, its nearest neighbor B on V^7 must have rank 2, and therefore lies in the manifold portion of V^7. It follows that the shortest geodesic from A to B is orthogonal to V^7, and since we saw in section 9 that the 5-cell fibres of N meet V^7 orthogonally along their boundaries, this geodesic must lie in the 5-cell fibre of N containing A.

Therefore B lies on the boundary of this 5-cell fibre, as claimed.

Remark. Because the 5-cell fibres of N are not round, the nearest singular neighbor B is typically *not* at the end of the ray from the center of the cell through A, as was true for 2×2 matrices. We will shortly state the classical theorem of Eckart and Young which describes this nearest singular neighbor explicitly in terms of singular values.

Matrix Decompositions

Singular value decomposition

Let A be an $n \times k$ matrix, thus representing a linear map $A\colon \mathbb{R}^k \to \mathbb{R}^n$.

We seek a matrix decomposition of A,

$$A = WDV^{-1},$$

where V is a $k \times k$ orthogonal matrix, where D is an $n \times k$ diagonal matrix,

$$D = \operatorname{diag}(d_1, d_2, \ldots, d_r), \quad \text{with } d_1 \geq d_2 \geq \cdots \geq d_r \geq 0,$$

with $r = \min(k, n)$, and where W is an $n \times n$ orthogonal matrix.

The message of this decomposition is that A takes some right angled k-dimensional box in $\mathbb{R}^k$ to some right angled box of dimension $\leq k$ in $\mathbb{R}^n$, with the columns of the orthogonal matrices V and W serving to locate the edges of the domain and image boxes, and the diagonal matrix D reporting expansion and compression of these edges (Figure 14). See Golub and Van Loan [1996] and Horn and Johnson [1991] for derivation of this singular value decomposition.

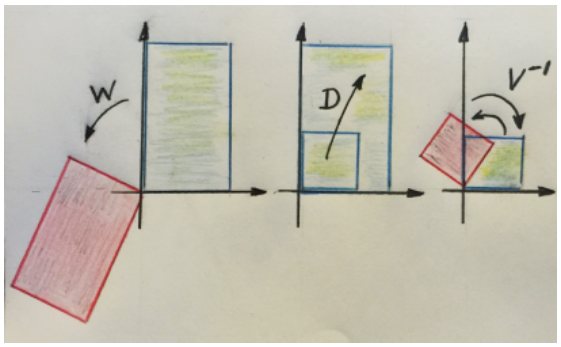

Figure 14: ***Singular value decomposition:*** $\boldsymbol{A = WDV^{-1}}$

Remarks. (1) Consider the map $A^TA\colon \mathbb{R}^k \to \mathbb{R}^k$, and note that

$$A^TA = (VDW^{-1})(WDV^{-1}) = VD^2V^{-1},$$

with eigenvalues $d_1^2, d_2^2, \ldots, d_r^2$ and if $r = n < k$, then also with $k-n$ zero eigenvalues. The orthonormal columns $\mathbf{v}_1, \mathbf{v}_2, \ldots, \mathbf{v}_k$ of V are the corresponding eigenvectors of A^TA, since for example

$$A^TA(\mathbf{v}_1) = VD^2V^{-1}(\mathbf{v}_1) = VD^2(1, 0, \ldots, 0) = V(d_1^2, 0, \ldots, 0) = d_1^2\mathbf{v}_1,$$

and likewise for $\mathbf{v}_2, \ldots, \mathbf{v}_k$.

(2) In similar fashion, consider the map $AA^T\colon \mathbb{R}^n \to \mathbb{R}^n$, note that

$$AA^T = (WDV^{-1})(VDW^{-1}) = WD^2W^{-1},$$

with eigenvalues $d_1^2, d_2^2, \ldots, d_r^2$, and if $r = k < n$, then also with $n-k$ zero eigenvalues. The orthonormal columns $\mathbf{w}_1, \mathbf{w}_2, \ldots, \mathbf{w}_n$ of W are the corresponding eigenvectors of AA^T.

(3) The singular value decomposition was discovered independently by the Italian differential geometer Eugenio Beltrami [1873] and the French algebraist Camille Jordan [1874a, b] , in response to a question about the bi-orthogonal equivalence of quadratic forms. Later, Erhard Schmidt [1907] introduced the infinite-dimensional analogue of the singular value decomposition and addressed the problem of finding the best approximation of lower rank to a given bilinear form.

Carl Eckart and Gale Young [1936] extended the singular value decomposition to rectangular matrices, and rediscovered Schmidt's 1907 theorem about approximating a matrix by one of lower rank.

(4) Since finding the singular value decomposition of a matrix A is equivalent to computing the eigenvalues and orthonormal eigenvectors of the symmetric matrices A^TA and AA^T, all of the computational techniques that apply to positive (semi)definite symmetric matrices apply, in particular the celebrated QR-algorithm, which was proposed independently by John Francis [1961] and Vera Kublanovskaya [1962]. Its later refinement, the *implicitly shifted QR algorithm*, was named one of the top ten algorithms of the 20th century by the editors of SIAM news (Cipra [2000]). For more historical details, we recommend Stewart [1993].

Polar decomposition

The ***polar decomposition*** of an $n \times n$ matrix A is the factoring

$$A = UP,$$

where U is orthogonal and P is symmetric positive semi-definite.

The message of this decomposition is that P takes some right angled n-dimensional box in $\mathbb{R}^n$ to itself, edge by edge, expanding and compressing some while perhaps sending others to zero, after which U moves the image box rigidly to another position (Figure 15).

See Golub and Van Loan [1996] and Horn and Johnson [1991] for derivation of this polar decomposition.

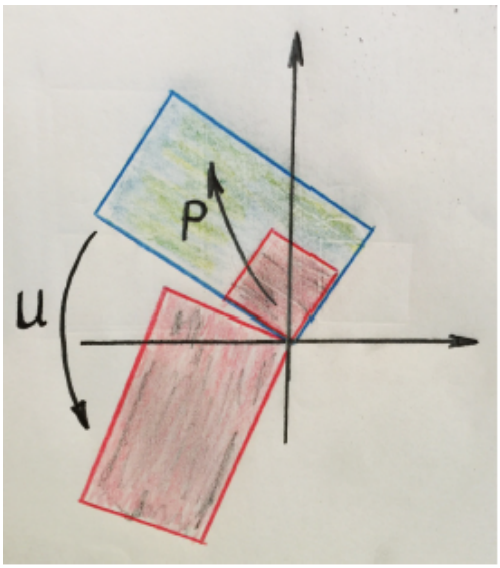

Figure 15: ***Polar decomposition: $A = UP$***

Remarks. (1) Existence of the polar decomposition follows immediately from the singular value decomposition for A:

$$A = WDV^{-1} = (WV^{-1})(VDV^{-1}) = UP.$$

Furthermore, if $A = UP$, then $A^T = P^T U^T = PU^{-1}$, and hence

$$A^T A = (PU^{-1})(UP) = P^2.$$

Now the symmetric matrix $A^T A$ is positive semi-definite, and has a unique symmetric positive semi-definite square root $P = \sqrt{A^T A}$.

(2) In the polar decomposition $A = UP$, the factor P is uniquely determined by A, while the factor U is uniquely determined by A if A is nonsingular, but not in general if A is singular.

(3) If $n = 3$ and A is nonsingular, with polar decomposition $A = UP$, and if we scale A to lie on $S^8(\sqrt{3})$, then P will also lie on that sphere, and the polar decomposition of A is just the product coordinatization of the open tubular neighborhoods N and N' of $SO(3)$ and $O^-(3)$.

(4) An $n \times n$ matrix A of rank r has a factorization $A = UP$, with U best of rank r and P symmetric positive semi-definite, and with both factors U and P uniquely determined by A and having the same rank r as A.

(5) Let A be a real nonsingular $n \times n$ matrix, and let $A = UP$ be its polar decomposition. Then U is the nearest orthogonal matrix to A, in the sense of minimizing the norm $\|A - V\|$ over all orthogonal matrices V.

(6) Let $A = UP$ be an $n \times n$ matrix of rank r with U best of rank r and P symmetric positive semi-definite. Then U is the nearest best of rank r matrix to A, in the sense of minimizing the norm $\|A - V\|$ over all best of rank r matrices V.

(7) The decomposition $A = UP$ is called ***right polar decomposition***, to distinguish it from the ***left polar decomposition*** $A = P'U'$. Given the right polar decomposition $A = UP$, we can write $A = UP = (UPU^{-1})U = P'U$ to get the left polar decomposition. If A is nonsingular, then the unique orthogonal factor U is the same for both right and left polar decompositions, but the symmetric positive semi-definite factors P and P' are not. No surprise about the orthogonal factor being the same, since in either case it is the unique element of the orthogonal group $O(n)$ closest to A.

(8) Léon Autonne [1902], in his study of matrix groups, first introduced the polar decomposition $A = UP$ of a square matrix A, where U is unitary and P is Hermitian, and quickly proved its existence.

The Nearest Singular Matrix

Theorem (Eckart and Young, 1936). ***Let A be an $n \times k$ matrix of rank r, with singular value decomposition $A = WDV^{-1}$, where V is a $k \times k$ orthogonal matrix, where D is an $n \times k$ diagonal matrix,***

$$D = \mathrm{diag}(d_1, d_2, \ldots, d_r, 0, \ldots, 0), \quad \textit{with } d_1 \geq d_2 \geq \ldots d_r > 0,$$

and where W is an $n \times n$ orthogonal matrix.
Then the nearest $n \times k$ matrix A' of rank $\leq r' < r$ is given by $A' = WD'V^{-1}$, with W and V as above, and with

$$D' = \mathrm{diag}(d_1, d_2, \ldots, d_{r'}, 0, \ldots, 0).$$

We illustrate this in Figure 16 in the setting of 3 x 3 matrices. In that figure, we start

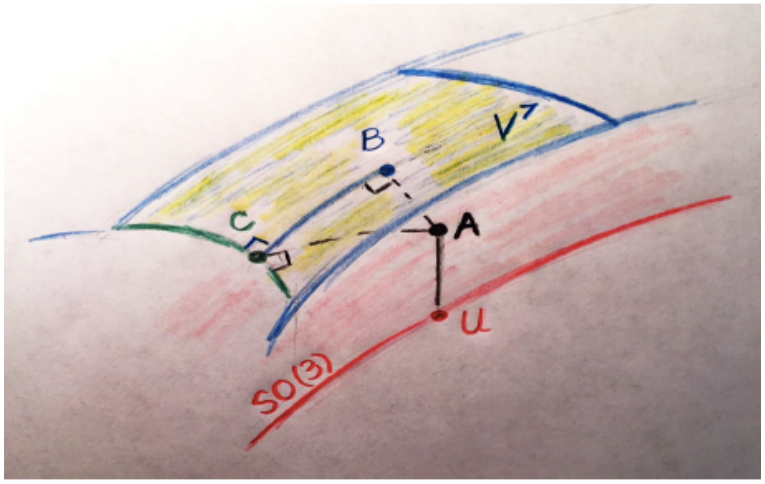

Figure 16: ***Nearest singular matrix***

with a 3×3 matrix A on $S^8(\sqrt{3})$, having positive determinant and thus lying within the tubular neighborhood N of $SO(3)$, with U its nearest orthogonal neighbor. If B is the nearest singular matrix on $S^8(\sqrt{3})$ to A, and C is the nearest rank 1 matrix on $S^8(\sqrt{3})$ to B, then C will also be the nearest rank 1 matrix there to A.

Principal component analysis

Consider the singular value decomposition $A = WDV^{-1}$ of an $n \times k$ matrix A, where V is a $k \times k$ orthogonal matrix, where D is an $n \times k$ diagonal matrix,

$$D = \mathrm{diag}(d_1, d_2, \ldots, d_r), \quad \text{with } d_1 \geq d_2 \geq \cdots \geq d_r \geq 0,$$

with $r = \min(k, n)$, and where W is an $n \times n$ orthogonal matrix.

Suppose that the rank of A is $s \leq r = \min(k, n)$, and that $s' < s$. Then from the Eckart-Young theorem, we know that the nearest $n \times k$ matrix A' of rank $\leq s' < s$ is given by $A' = WD'V^{-1}$, with W and V as above, and with

$$D' = \mathrm{diag}(d_1, d_2, \ldots, d_{s'}).$$

The image of A' has the orthonormal basis $\{\mathbf{w}_1, \mathbf{w}_2, \ldots, \mathbf{w}_{s'}\}$, which are the first s' columns of the matrix W.

The columns of W are the vectors $\mathbf{w}_1, \mathbf{w}_2, \ldots$, and are known as the ***principal components*** of the matrix A , and the first s' of them span the image of the best rank s' approximation to A.

If the matrix A is used to collect a family of data points, and these data points are listed as the columns of A, then the orthonormal columns of W are regarded as the principal components of this family of data points.

But if the data points are listed as the rows of A, then it is the orthonormal columns of V which serve as the principal components.

Remark. Principal Component Analysis began with Karl Pearson [1901]. He wanted to find the line or plane of closest fit to a system of points in space, in which the measurement of the locations of the points are subject to errors in any direction.

His key observation was that to achieve this, one should seek to minimize the sum of the squares of the perpendicular distances from all the points to the proposed line or plane of best fit. The best fitting line is what we now view as the first principal component, described earlier (Figure 17).

The actual term "*principal component*" was introduced by Harold Hotelling [1933].

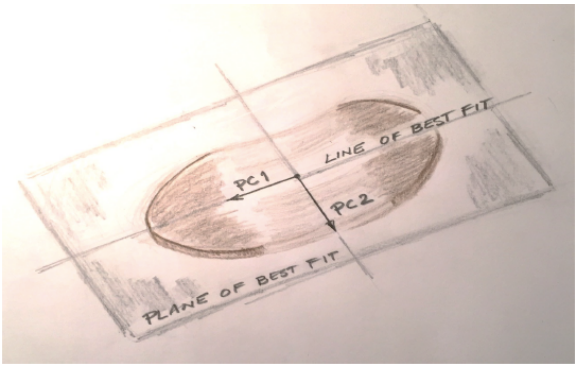

Figure 17: ***Principal components 1 and 2***

For further reading about the history of these matrix decompositions, we recommend Horn and Johnson [1991], pages 134–140, and Stewart [1993] as excellent resources.

Applications of nearest orthogonal neighbor

The orthogonal Procrustes problem

Let $P = \{\mathbf{p}_1, \mathbf{p}_2, \ldots, \mathbf{p}_k\}$ and $Q = \{\mathbf{q}_1, \mathbf{q}_2, \ldots, \mathbf{q}_k\}$ be two ordered sets of points in Euclidean n-space $\mathbb{R}^n$. We seek a rigid motion U of n-space which moves P as close as possible to Q, in the sense of minimizing the ***disparity*** $d_1^2 + d_2^2 + \cdots + d_k^2$ between $U(P)$ and Q, where $d_i = \|U(\mathbf{p}_i) - \mathbf{q}_i\|$.

It is easy to check that if we first translate the sets P and Q to put their centroids at the origin, then this will guarantee that the desired rigid motion U also fixes the origin, and so lies in $O(n)$. We assume this has been done, so that the sets P and Q have their centroids at the origin.

Then we form the $n \times k$ matrices A and B whose columns are the vectors $\mathbf{p}_1, \mathbf{p}_2, \ldots, \mathbf{p}_k$ and $\mathbf{q}_1, \mathbf{q}_2, \ldots, \mathbf{q}_k$, and we seek the matrix U in $O(n)$ which minimizes the disparity $d_1^2 + d_2^2 + \cdots + d_k^2 = \|UA - B\|^2$ between $U(P)$ and Q.

We start by expanding

$$\langle UA - B\,,\, UA - B\rangle = \langle UA\,,\, UA\rangle - 2\langle UA\,,\, B\rangle + \langle B, B\rangle.$$

Now $\langle UA\,,\, UA\rangle = \langle A, A\rangle$ which is fixed, and likewise $\langle B, B\rangle$ is fixed, so we want to *maximize* the inner product $\langle UA\,,\, B\rangle$ by appropriate choice of U in $O(n)$. But

$$\langle UA\,,\, B\rangle = \langle U\,,\, BA^T\rangle,$$

and so, reversing the above steps, we want to *minimize* the inner product

$$\langle U - BA^T\,,\, U - BA^T\rangle,$$

which means that we are seeking the orthogonal transformation U which is closest to BA^T in the space of $n \times n$ matrices.

The above argument was given by Peter Schönemann [1966] in his PhD thesis at the University of North Carolina.

When $n \geq 3$, we don't have a simple explicit formula for U, but it is the orthogonal factor in the polar decomposition

$$BA^T = UP = P'U.$$

Visually speaking, if we scale BA^T to lie on the round $n^2 - 1$ sphere of radius $\sqrt{n}$ in n^2-dimensional Euclidean space $\mathbb{R}^{n^2}$, then U is at the center of the cross-sectional cell in the tubular neighborhood of $O(n)$ which contains BA^T, and is unique if $\det(BA^T) \neq 0$.

A least squares estimate of satellite attitude

Let $P = \{\mathbf{p}_1, \mathbf{p}_2, \ldots, \mathbf{p}_k\}$ be unit vectors in 3-space which represent the direction cosines of k objects observed in an earthbound fixed frame of reference, and $Q = \{\mathbf{q}_1, \mathbf{q}_2, \ldots, \mathbf{q}_k\}$ the direction cosines of the same k objects as observed in a satellite fixed frame of reference. Then the element U in $SO(3)$ which minimizes the disparity between $U(P)$ and Q is a least squares estimate of the rotation matrix which carries the known frame of reference into the satellite fixed frame at any given time. See Wahba [1966].

Errors incurred in computation of U can result in a loss of orthogonality, and be compensated for by moving the computed U to its nearest orthogonal neighbor.

Procrustes best fit of anatomical objects

The challenge is to compare two similar anatomical objects: two skulls, two teeth, two brains, two kidneys, and so forth.

Anatomically corresponding points (*landmarks*) are chosen on the two objects, say the ordered set of points $P = \{\mathbf{p}_1, \mathbf{p}_2, \ldots, \mathbf{p}_k\}$ on the first object, and the ordered set of points $Q = \{\mathbf{q}_1, \mathbf{q}_2, \ldots, \mathbf{q}_k\}$ on the second object. They are translated to place their centroids at the origin, and then the Procrustes procedure is applied by seeking a rigid motion U of 3-space so as to minimize the disparity $d_1^2 + d_2^2 + \cdots + d_k^2$ between $U(P)$ and Q , where $d_i = \|U(\mathbf{p}_i) - \mathbf{q}_i\|$.

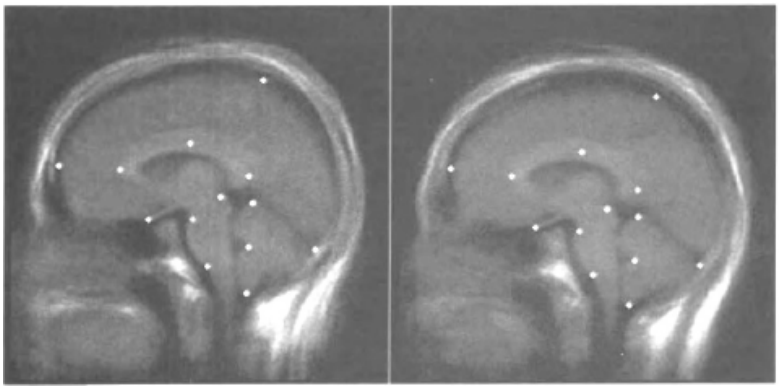

Figure 18: ***Brain scans***

In Figure 18, the left brain slice is actually an average over a group of doctors, and the right slice an average over a group of patients, each with 13 corresponding landmark points, from the paper by Bookstein [1997].

If size is not important in the comparison of two shapes, then it can be factored out

by scaling the two sets of landmarks, $P = \{\mathbf{p}_1, \mathbf{p}_2, \ldots, \mathbf{p}_k\}$ and $Q = \{\mathbf{q}_1, \mathbf{q}_2, \ldots, \mathbf{q}_k\}$, so that $\|\mathbf{p}_1\|^2 + \cdots + \|\mathbf{p}_k\|^2 = \|\mathbf{q}_1\|^2 + \cdots + \|\mathbf{q}_k\|^2$.

For modifications which allow comparison of any number of shapes at the same time, see for example Rohlf and Slice [1990].

The effectiveness of this Procrustes comparison naturally depends on appropriate choice and placement of the landmark points, and leads one to seek an alternative approach which does not depend on this. To that end, see Lipman, Al-Aifari and Daubechies [2013] in which the authors propose a continuous Procrustes distance, and then prove that it provides a metric for the space of "shapes" of two-dimensional surfaces embedded in three-space.

Facial recognition and eigenfaces

We follow Sirovich and Kirby [1987] in which the principal components of the data base matrix of facial pictures are suggestively called ***eigenpictures***.

The authors and their team assembled a file of 115 pictures of undergraduate students at Brown University. Aiming for a relatively homogeneous population, these students were all smooth-skinned caucasian males. The faces were lined up so that the same vertical line passsed through the symmetry line of each face, and the same horizontal line through the pupils of the eyes. Size was normalized so that facial width was the same for all images.

Each picture contained $128 \times 128 = 2^{14} = 16,384$ pixels, with a grey scale determined at each pixel. So each picture was regarded as a single vector $\varphi^{(n)}$, $n = 1, 2, \ldots, 115$, called a ***face***, in a vector space of dimension 2^{14}.

The challenge was to find a low-dimensional subspace of best fit to these 115 faces, so that a person could be sensibly recognized by the projection of his picture into this subspace.

To make sure that the subspace passes through the origin (i.e., is a linear rather than affine subspace), the data is adjusted so that its average is zero, as follows.

Let $\langle\varphi\rangle = (1/M)\sum_{n=1}^{M} \varphi^{(n)}$ be the average face, where $M = 115$, and then let $\phi^{(n)} = \varphi^{(n)} - \langle\varphi\rangle$ be the deviation of each face from the average. The authors refer to each such deviation ϕ as a ***caricature***. Figure 19 shows a sample face, and its caricature.

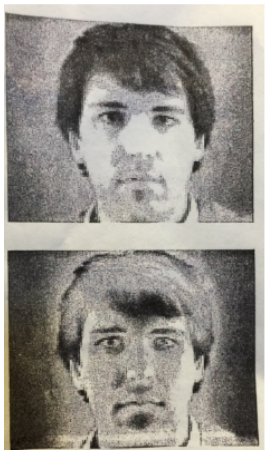

Figure 19: ***Sample face and caricature***

The collection of caricatures $\phi^{(n)},\ n = 1, 2, \ldots, 115$ was then regarded as a $2^{14} \times 115$ matrix A, with each caricature appearing as a column of A.

If the singular value decomposition of A is $A = WDV^{-1}$, with W a $2^{14} \times 2^{14}$ orthogonal matrix,

$$D = \text{diag}(d_1, d_2, \ldots, d_{115}) \quad \text{with } d_1 \geq d_2 \geq \cdots \geq d_{115} \geq 0$$

a $2^{14} \times 115$ diagonal matrix, and V a 115×115 orthogonal matrix, then the orthonormal columns $\mathbf{w}_1, \mathbf{w}_2, \ldots, \mathbf{w}_{2^{14}}$ of W are the principal components of the matrix A.

It was found that the first 100 principal components of A span a subspace sufficiently large to recognize any of the faces $\varphi^{(n)}$ by projecting its caricature into this subspace and then adding back the average face:

$$\varphi^{(n)} \sim \langle \varphi \rangle + \sum_{k=1}^{100} \langle \phi^{(n)}\ ,\ \mathbf{w}_k \rangle\, \mathbf{w}_k.$$

Figure 20 shows the first eight eigenpictures starting at the upper left, moving to the right, and ending at the lower right, in which each picture is cropped to focus on the eyes and nose. Since the eigenpictures can have negative entries, a constant was added to all the entries to make them positive for the purpose of viewing

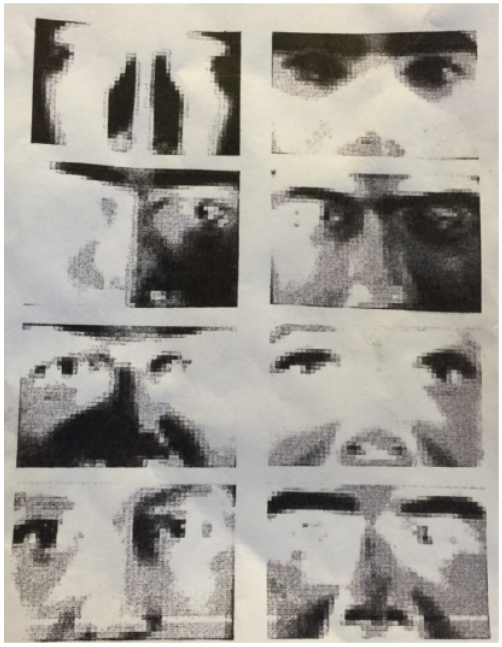

Figure 20: ***First eight eigenfaces***

Figure 21 shows a sample face, correspondingly cropped, and Figure 22 shows the

Figure 21: ***Cropped sample face***

approximations to that sample face, using 10, 20, 30 and 40 eigenpictures.

Figure 22: ***Approximations to sample face***

After working with the initial group of 115 male students, the authors tried out the recognition procedure on one more male student and two females, using 40 eigenpictures, with errors of 7.8%, 3.9%, and 2.4% in these three cases.

Remarks.

(1) In the pattern recognition literature, the Principal Component Analysis method used in this paper is also known as the Karhunen-Loeve expansion.

(2) Another very informative and nicely written paper on this approach to facial recognition is Turk and Pentland [1991]. The section of this paper on *Background and Related Work* is a brief but very interesting survey of alternative approaches to computer recognition of faces. An overview of the literature on face recognition is given in Zhao et al [2003].

Principal component analysis applied to interest rate term structure

How does the interest rate of a bond vary with respect to its *term*, meaning time to maturity? The answer involves one of the oldest and best known applications of Principal Components Analysis (PCA) to the field of economics and finance, originating in the work of Litterman and Scheinkman [1991].

To begin, economists plot the interest rate for a given bond against a variety of different maturities, and call this a ***yield curve***. Figure 23 shows such a curve for US Treasury bonds from an earlier date, when interest rates were higher than they are now.

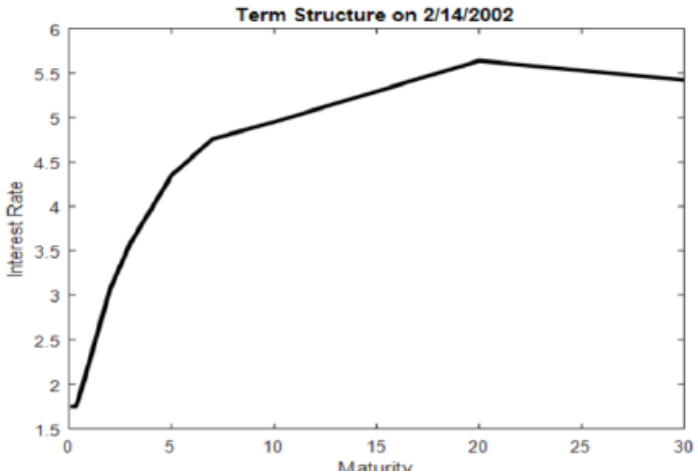

Figure 23: ***Yield curve***

Predicting the relation shown by such a curve can be crucial for investors trying to determine which assets to invest in, and for governments who wish to determine the best mix of Treasury maturities to auction on any given day. For this reason, a number of investigators have tried to understand whether there are common factors embedded in the term structure. In particular, identifying whether there are factors which affect all interest rates equally, or which affect interest rates for bonds of certain maturities but not of others, is important for understanding how the term structure behaves.

To help understand how these questions are answered, we replicated the methodology in the Litterman and Scheinkman paper, using a newer data set which gives the daily interest rate term structure for US Treasury bonds over a long span of time, 2,751 days between 2001 and 2016. For each of these days, we recorded the interest rates for bonds of 11 different maturities: 1, 3 and 6 months, and 1, 2, 3, 5, 7, 10, 20 and 30 years. Each data vector is an 11-tuple of interest rates, which we collect as the rows of a $2,751 \times 11$ matrix.

The average of the rows is depicted graphically in Figure 24. We subtracted this average from each of the rows, and called the resulting matrix A. The rows of A are our *adjusted data vectors*, which now add up to zero.

Let $A = WDV^{-1}$ be the singular value decomposition of A, where V is an 11×11 orthogonal matrix, D is a $2,751 \times 11$ diagonal matrix, and W is a $2,751 \times 2,751$ orthogonal matrix. Since the data points are the *rows* of A, the principal components are the 11 orthonormal columns of V.

These principal components reveal the line of best fit, the plane of best fit, the

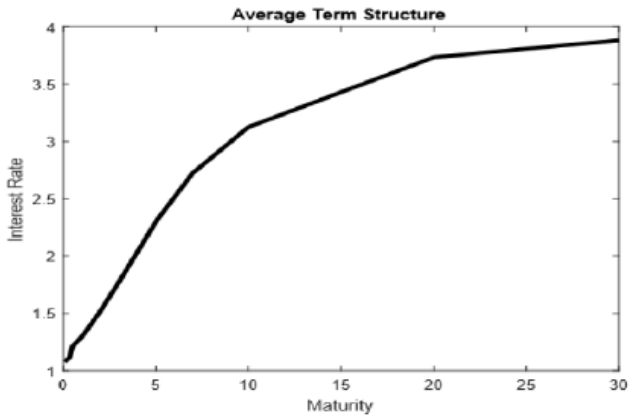

Figure 24: ***Average yield curve***

3-space of best fit, and so forth for our 2,751 data points. They were obtained using the PCA package of MATLAB. The first three principal components are shown graphically in Figure 25. The first principal component is more constant than the

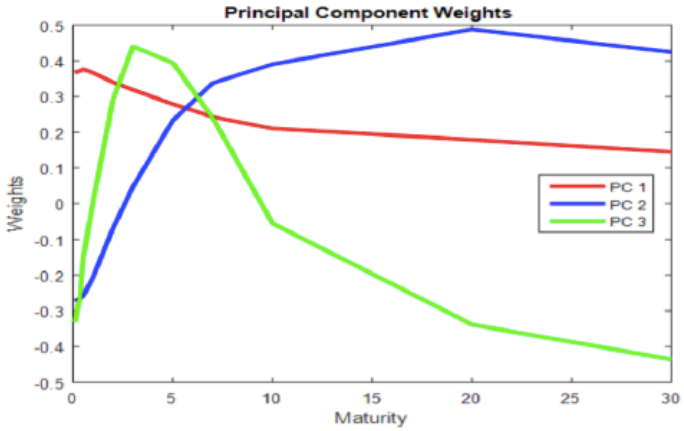

Figure 25: ***Principal components of A***

other two, and captures the fact that most of the variation in term structures comes from changes which affect the levels of all yields.

The second most important source of variation in term structure comes from the second principal component, which reflects changes that most affect yields on bonds of longer maturities, while the third principal component reflects changes that affect medium term yields the most. These features of the first three principal components were called *level*, *steepness*, and *curvature* in the foundational paper by Litterman and Scheinkman.

In Figure 26, the black curve is the term structure on 2/14/2002, duplicating the first figure in this section. We subtract the average term structure from this particular one, project the difference onto the one-dimensional subspaces spanned in turn by the first three principal components, and show these projections below in red, blue and green. Finally, we sum up these three projections, add back the average term structure, show the result in purple, and see how closely this purple curve approximates the black curve we started with.

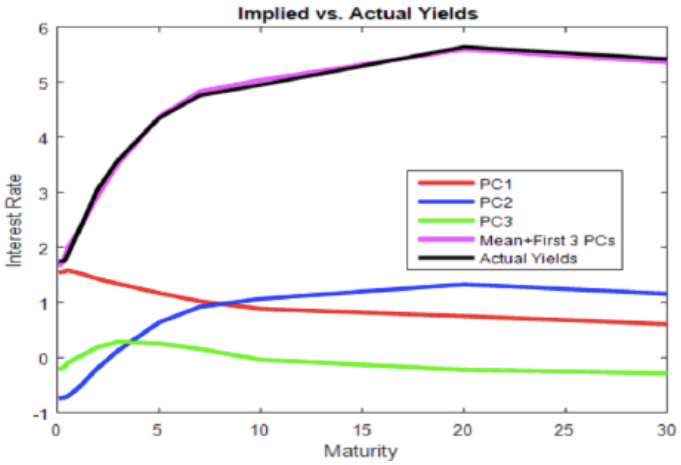

Figure 26: ***Approximation of a yield curve by its first three principal components***

REFERENCES

1873 E. Beltrami, *Sulle funzioni bilineari*, Giornali di Mat. ad Uso degli Studenti Delle Universita, 11, 98–106

1874a C. Jordan, *Memoire sur les formes bilineares*, J. Math. Pures Appl., 2nd series, 19, 35–54

1874b C. Jordan, *Sur la reduction des formes bilineares*, Comptes Rendus de l'Academie Sciences, Paris 78, 614–617

1901 Karl Pearson, *On Lines and Planes of Closest Fit to Systems of Points in Space*, Philosophical Magazine 2, 559–572.

1902 L. Autonne, *Sur les groupes lineaires, reels et orthogonaux*, Bull. Soc. Math. France, 30, 121–134

1907 E. Schmidt, *Zur Theorie des linearen und nichlinearen Integral gleichungen, I Teil. Entwicklung willkurlichen Funktionen nach System vorgeschriebener*, Math. Ann. 63, 433 – 476

1933 H. Hotelling, *Analysis of a complex of statistical variables into principal components*, J. Ed. Psych, 24, 417 – 441 and 498 – 520

1936 C. Eckart and G. Young, *The approximation of one matrix by another of lower rank*, Psychometrika, I, 211 – 218.

1947 Kari Karhunen, *Uber lineare Methoden in der Wahrscheinlichkeitsrechnung*, Ann. Acad. Sci. Fennicae, Ser. A. I. Math-Phys 37, 1–79.

1961 John Francis, *The QR transformation*, parts I and II, Computer J. Vol. 4, 265–272 and 332–345.

1962 Vera Kublanovskaya, *On some algorithms for the solution of the complete eigenvalue problem*, USSR Comput. Math. and Math. Physics. vol 1, 637–657.

1966 Peter H. Schönemann, *A generalized solution of the orthogonal Procrustes problem*, Psychometrika, Vol. 31, No. 1, March, 1 – 10.

1966 Grace Wahba, *A Least Squares Estimate of Satellite Attitude*, SIAM Review, Vol. 8, No. 3, 384 – 386.

1976 Wolfgang Kabsch, *A solution for the best rotation to relate two sets of vectors*, Acta Crystallographica 32, 922, with a correction in 1978, *A discussion of the solution for the best rotation to relate two sets of vectors*, Ibid, A-34, 827–828.

1980 H. Blaine Lawson, *Lectures on Minimal Submanifolds*, Publish or Perish Press.

1985 Roger Horn and Charles Johnson, *Matrix Analysis*, Cambridge University Press.

1986 Nicholas J. Higham, *Computing the polar decomposition – with applications*, SIAM J. Sci. Stat. Comput. Vol. 7, No. 4 October, 1160 – 1174.

1987 L. Sirovich and M. Kirby, *Low-dimensional procedure for the characterization of human faces*, J. Optical Society of America, Vol. 4, No. 3, 519 – 524,

1990 F. James Rohlf and Dennis Slice, *Extensions of the Procrustes method for the optimal superimposition of landmarks*, Syst. Zool. 39 (1), 40 – 59.

1991 Roger Horn and Charles Johnson, *Topics in Matrix Analysis*, Cambridge University Press.

1991 Robert Litterman and José Scheinkman, *Common factors affecting bond returns*, J. Fixed Income, June, 54 – 61.

1991 Matthew Turk and Alex Pentland, *Eigenfaces for Recognition*, Journal of Cognitive Neuroscience, Vol. 3, No. 1, 71 – 86.

1993 G.W. Stewart, *On the early history of the singular value decomposition*, SIAM Review, Vol. 35, No. 4, 551 – 566

1996 Gene Golub and Charles Van Loan, *Matrix Computations*, Third Edition, Johns Hopkins University Press.

1997 Fred L. Bookstein, *Biometrics and brain maps: the promise of the Morphometric Synthesis*, in S. Kowlow and M. Huerta, eds., *Neuroinformatics: An Overview of the Human Brain Project*, Progress in Neuroinformatics, Vol. 1, 203 – 254.

2000 Barry Cipra, *The Best of the 20th Century: Editors Name Top 10 Algorithms*, SIAM News, Vol. 33, No. 4, 1–2.

2002 Allen Hatcher, *Algebraic Topology*, Cambridge University Press.

2003 W. Zhao, R. Chellappa, P.J. Phillips and A. Rosenfeld, *Face Recognition: A Literature Survey*, ACM Computing Surveys, Vol. 35, No. 4, 399 – 458.

2009 G. H. Golub and F. Uhlig, *The QR algorithm: 50 years later its genesis by John Francis and Vera Kublanovskaya and subsequent developments*, IMA J. Numer. Anal. Vol. 29, 467–485.

2011 David S. Watkins, *Francis's Algorithm*, American Mathematical Monthly Vol. 118, May, 387–403.

2013 Yaron Lipman, Reema Al-Aifari and Ingrid Daubechies, *The continuous Procrustes distance between two surfaces*, Comm. Pure Appl. Math. 66, 934 – 964,

University of Pennsylvania
Philadelphia, PA 19104

Dennis DeTurck: *deturck@math.upenn.edu*
Amora Elsaify: *aelsaify@wharton.upenn.edu*
Herman Gluck: *gluck@math.upenn.edu*
Benjamin Grossmann: *bwg25@drexel.edu*
Joseph Hoisington: *jhois@math.upenn.edu*
Anusha M. Krishnan: *anushakr@math.upenn.edu*
Jianru Zhang: *jianruzh@math.upenn.edu*